Measurements of the Vertical Coherence Length in Neutron Interferometry

D. A. Pushin,[1,*] M. Arif,[2] M. G. Huber,[3] and D. G. Cory[1]

[1]*Department of Nuclear Science and Engineering, Massachusetts Institute of Technology, Cambridge, Massachusetts, USA*
[2]*National Institute of Standards and Technology, Gaithersburg, Maryland, USA*
[3]*Department of Physics, Tulane University, New Orleans, Louisiana, USA*

(Received 19 March 2008; published 26 June 2008)

The study and use of macroscopic quantum coherence requires long coherence lengths. Here we describe an approach to measuring the vertical coherence length in neutron interferometry, along with improvements to the NIST interferometer that led to a measured coherence length of 790 Å. The measurement is based on introducing a path separation and measuring the loss in contrast as this separation is increased. The measured coherence length is consistent with the momentum distribution of the neutron beam. Finally, we demonstrate that the loss in contrast with beam displacement in one leg of the interferometer can be recovered by introducing a corresponding displacement in the second leg.

DOI: 10.1103/PhysRevLett.100.250404 PACS numbers: 03.75.Dg, 03.65.−w, 42.50.−p

Introduction.—We wish to develop neutron interferometery as a robust practical example of a macroscopic coherent device with potential application to quantum information processing (QIP) and condensed matter physics. Interferometry is one of the most direct measures of quantum interference [1–4]. Having an interferometer with a long coherence length opens up the possibilities of using interferometry for new experiments and studies that are not easily accessible by other approaches. Increases in the coherence length also improve both the interferometer contrast and the precision of measurements. In particular a long vertical coherence length would allow useful implementations of Fourier spectroscopy [5] with applications in condensed matter and biology. Beyond such applications a long coherence length would also benefit foundational physics questions. Here a long coherence length permits studies of macroscopical quantum interference [6], since increasing the coherence length moves the description of interferometry towards a more plane-wave picture and permits simple studies of decoherence. Here we describe modifications to the National Institute of Standards and Technology (NIST) neutron interferometer that increased the coherence length (l_c) and we describe a method to directly measures the spatial coherence.

The coherence length describes the spatial extent over which coherent information is preserved in interferometry [1]. In a neutron interferometer [7] the coherence length is a function of the quality of the single crystal, the momentum distribution of the incoming neutron beam, and a variety of environmental contributions including temperature gradients and vibrations. Generally three coherent lengths are identified [8], the transverse coherence length, the vertical, and the longitudinal (see Fig. 1). Here we explore the vertical component in a system where the coherence length is primary limited by the incoming beam characteristics: the coherence length is limited by Heisenberg's uncertainty relation $l_c = 1/(2\delta k)$, where δk is momentum spread. To understand this limit we study the contrast associated with a wave packet composed from an incident distribution of plane waves corresponding to a distribution of neutron momenta in the vertical direction. The measurement of the coherent length is a direct measurement of the spatial extent of this wave packet. Note that the observed high contrast with a beam size of several mm indicates that any irregularities in the interferometer crystal have a small and weak influence on the coherence length. In the previous measurements of the coherence function [8] in a low coherence regime the coherence could be partially recovered by postselection methods. In our measurement we will not need to rely on postselection. The coherence (l_c) will be revealed by a simple projective measurement.

Experiment.—Neutron interferometery is a practical example of macroscopic quantum coherence [9]. We will describe this via a neutron wave function over a Mach-Zehnder interferometer. At the first blade the neutrons are split by Bragg scattering into two paths. The neutron wave function is $|\text{path}, \mathbf{p}\rangle$, where a neutron with momentum $\mathbf{p}$ spans *path I* and *path II* (Fig. 1). The phases that the neutron accumulates over each path are experimentally controlled via rotation of the phase flag (Fig. 1).

The measurements were made at the Neutron Interferometer and Optical Facility (NIOF) at the National Institute of Standards and Technology [10]. It consists of a perfect Si-crystal neutron interferometer shown in Fig. 1 with high phase contrast (>80%). The existing interferometer was machined from a silicon single crystal ingot and operates on a cold neutron beam ($E = 11.1$ meV, $\lambda = 0.271$ nm). Detailed descriptions of the facility can be found in Refs. [7,11].

Special care needs to be taken to increase the coherence length. We need high phase stability and high intensity to limit the total measurement time. The phase stability is influenced by environmental noise such as vibrations, acoustic noise, and temperature fluctuations. The NIOF at NIST has very good isolation from vibrations and

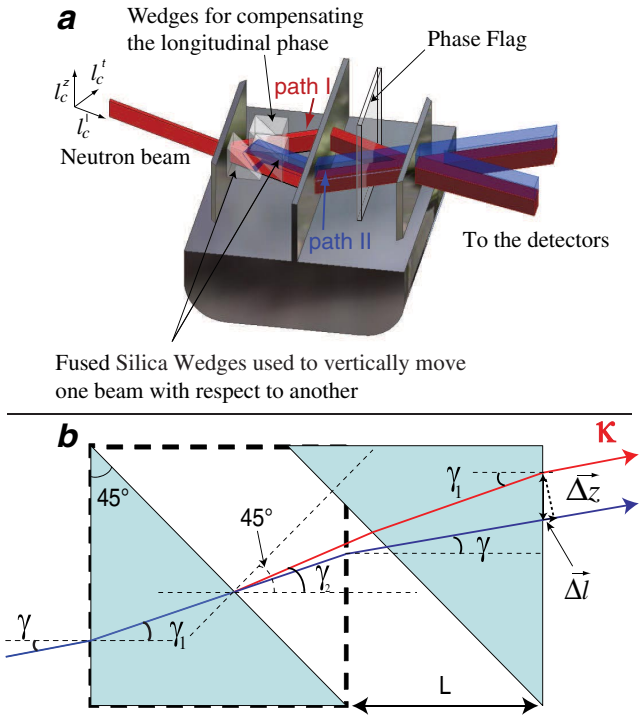

FIG. 1 (color online). (a) A schematic diagram of the coherence length experiment. A neutron beam, entering left, is coherently divided via Bragg diffraction at the first blade of the neutron interferometer into two paths (paths I and II). The phases that the neutron accumulates over each path are experimentally controlled by rotating the phase flag. In each path we install two 45° prisms, which at 0 separation form a cube. By separating the prisms we shift the neutron beams in path I and II vertically with respect to each other. As expected we observe a loss in contrast with displacement, Δz. (b) A schematic diagram of the neutron paths through the prisms. For comparison here we show two beam paths. The upper path corresponds to the neutron passing through the separated prisms, and the lower path through the prisms in a cube. The neutron beam enters from the left and depending on the separation between the prisms is shifted vertically. The angles shown in the figure are described in the text.

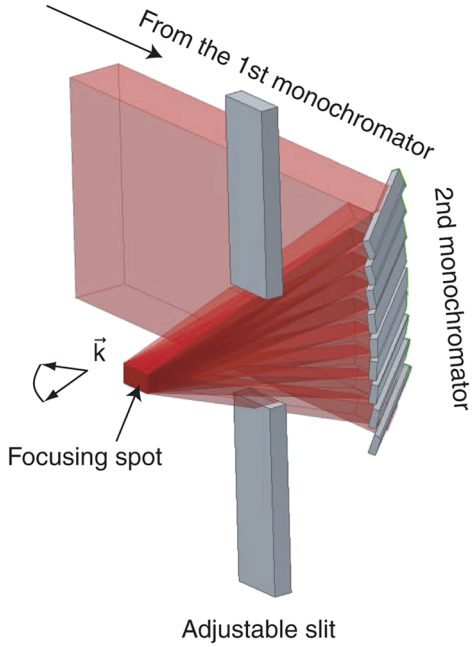

FIG. 2 (color online). A schematic diagram of the second monochromator. It consists of 9 PG blades and can focus the neutron beam to a smaller spot. By adjusting slit size after the second monochromator we can change the vertical momentum distribution.

acoustic noise [10]. In order to increase the phase stability over a longer period of time care was taken to control both the temperature and temperature gradients within the interferometer enclosure. Even a temperature gradient as small as 1 mK over 10 cm will shift interferometer blades by a few angstroms with respect to each other and result in a large phase change. The interferometer is housed in an aluminum enclosure and all heat sources (i.e. motors) are placed outside this enclosure. We installed two PT-100 calibrated thermometers in the enclosure (one in close vicinity of the neutron interferometer) to monitor both the absolute temperature and the gradient. A set of heaters were installed to set the temperature to near room temperature. Using a PID temperature controller we were able to maintain the temperature of the enclosure to within 5 mK, this dramatically improved the phase stability of our system.

In order to increase the intensity we used the second crystal of a parallel geometry double crystal monochromator as a focusing device. This crystal consists of 9 pyrolytic graphite (PG) blades shown in Fig. 2. Each blade can be independently adjusted to focus the neutron beam vertically on the first blade of the interferometer. While focusing the beam we try to keep the beam profile uniform. The focused beam provides much higher (about $\times 9$) intensity and significantly reduces the measurement time. As expected, the focused beam (bigger δk_z vertical momentum spread) corresponds to a smaller coherent length ($l_c^z \propto 1/\delta k_z$).

A pair of fused silica (90° angle, 15 mm side size) prisms forming a cube were placed in each path of the interferometer. As the prisms in one path are separated the neutron beam in that path is shifted vertically in a well controlled fashion. In addition to being displaced a phase shift is introduced into the wave function. This phase turns out to be quite small and its effects are not observed in our measurements so we will suppress it in the description that follows. However, our simulations do include this phase.

Consider a neutron as a plane wave with wave vector $\mathbf{k}$. If this vector $\mathbf{k}$ is not perpendicular to the vertical coordinate of the interferometer, then on passing through the prisms the vertical shift of the neutron beam will produce an additional phase shift of $\mathbf{k}\boldsymbol{\Delta l} = k_z \Delta z$ (it can be seen in the zoom in Fig. 1(b) that if at the edge of the prism the phases for two beams are the same, then due to nonzero k_z there will be phase shift $k_z \Delta z$ between these beams). The

wave function of a neutron over the interferometer is

$$\Psi = e^{i\mathbf{k}\mathbf{r}} e^{i\phi_1} C_1 |\mathrm{I}\rangle + e^{i\mathbf{k}(\mathbf{r}+\Delta\mathbf{z})} e^{i\phi_2} C_2 |\mathrm{II}\rangle, \quad (1)$$

where ϕ_1 and ϕ_2 are the phases over *path I* and *path II* in the absence of the prisms. The coefficients C_1 and C_2 are parameters of the neutron interferometer that account for the attenuation and scattering losses of the neutron beam due to interferometer crystal.

The vertical shift from the prisms is well described by introducing the index of refraction of the neutron

$$n = \frac{K_{\mathrm{inside}}}{k_0} \approx 1 - \lambda^2 \frac{N b_c}{2\pi}, \quad (2)$$

where b_c is the coherent scattering length, N is the atom density, K_{inside} is the wave vector of the neutron inside the prisms, k_0 is the wave vector of the incident neutron and we have ignored the reactive cross section. The vertical beam shift due to the sets of prisms is

$$\Delta\mathbf{z} = \Delta z_m (1 + \tan\gamma_1) - L\tan\gamma, \quad (3)$$

where $\Delta z_m = L\cos 45^\circ \sin\gamma_2 / \sin(45^\circ - \gamma_2) = L\tan\gamma_2/(1+\tan\gamma_2)$ is the vertical shift of the neutron beam in between the prisms in *path II*. Because $\tan\gamma = k_z/k$ and $\tan\gamma_1 \approx k_z/(nk)$ we can rewrite $\Delta\mathbf{z}$ for small angles as

$$\Delta\mathbf{z} \approx L\Delta n\left(1 - 2\frac{k_z}{k}\right). \quad (4)$$

The measured contrast originates from the constructive interference of the two paths as described by the projection operator for the O beam

$$P_O = \tfrac{1}{2}(|\mathrm{I}\rangle + |\mathrm{II}\rangle)(\langle \mathrm{I}| + \langle \mathrm{II}|). \quad (5)$$

The intensity in the direct beam direction is

$$I_O = \langle \Psi | P_O | \Psi \rangle. \quad (6)$$

For an incoherent sum of plane waves, the intensity on the detector is

$$\begin{aligned} I_O(\phi_0) &= \int \rho(k_z) \langle \Psi | P_O | \Psi \rangle dk_z \\ &= \int \rho(k_z) \left(\frac{1}{2}(C_1^2 + C_2^2) \right. \\ &\quad \left. + C_1 C_2 \cos(\phi_0 + k_z \Delta z) \right) dk_z, \end{aligned} \quad (7)$$

where $\rho(k_z)$ is the neutron vertical momentum distribution. The contrast is contained in the second term of the integral and the loss of contrast is a result of averaging over the momentum distribution.

Figure 3(a) shows the distribution of the vertical momentum for the incoming beam. The beam break consists of a first pyrolytic graphite (PG) monochromator followed by a set of 9 PG crystals that focus beam ($\lambda_n = 2.71$ Å) in the vertical direction at the input of the interferometer. The measured distribution corresponds to a sum of nine distributions that are offset from each other by the mean momentum from the individual graphite blades of the focusing monochromator. Figure 3(b) shows a series of measurements: the contrast versus the path separation $k_z\Delta z$ with all 9 blades; the contrast for the central 5 blades; and the contrast for the central most blade. As expected the contrast length increases as we narrow the momentum distribution of the incoming neutron beam. Notice that in the narrowest case the observed contrast remains up to 1000 Å vertical separation of the paths. Here we also show with solid lines the contrast curves obtained by approximating

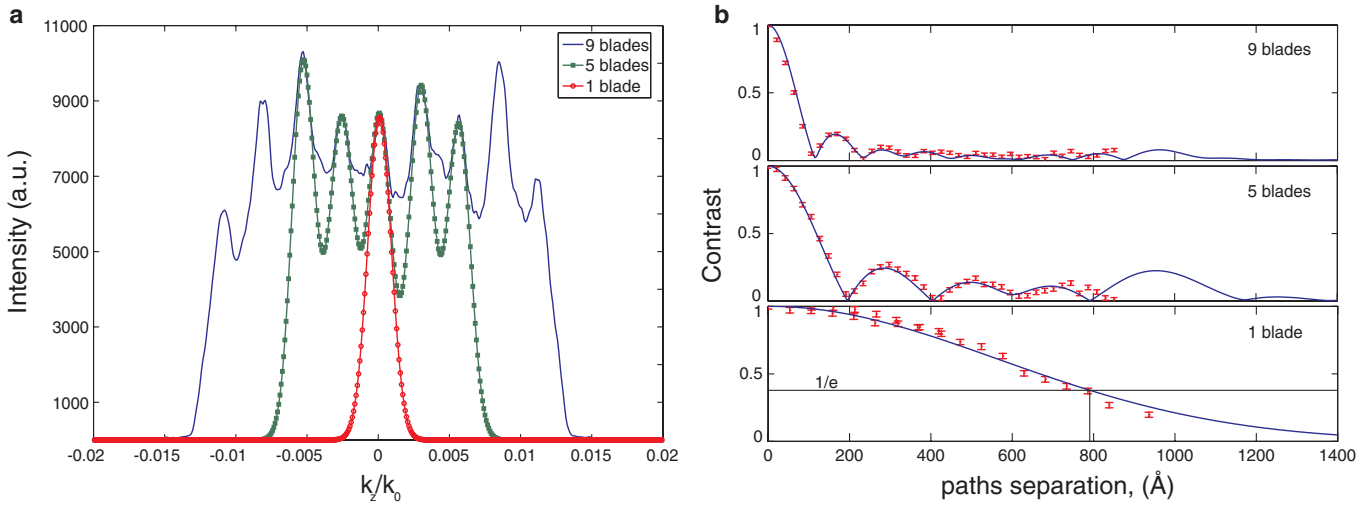

FIG. 3 (color online). (a) Vertical momentum distribution for the incoming neutron beam. The 9-blade distribution was measured and the 5 and 1 blades distributions are obtained by a simple model of a sum of displaced Gaussians. (b) Contrast plots for three different vertical beam divergences. In each subplot data are shown as closed circles. The lines are contrast curves derived as a sum of plane waves using the vertical momentum distribution (k_z) shown in (a). The data in (b) are very closely described by this approach.

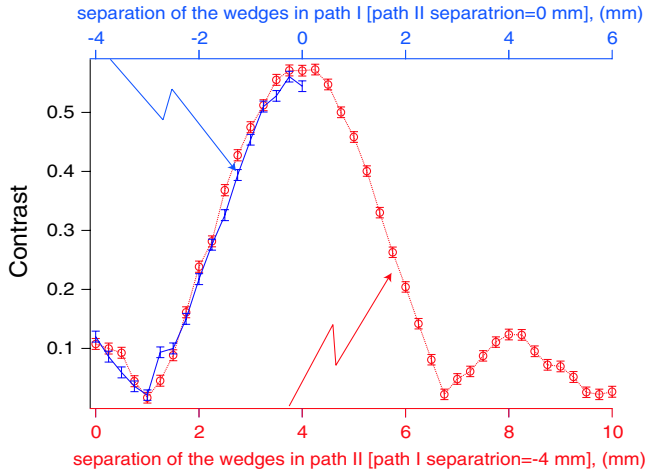

FIG. 4 (color online). Contrast plot for two cases: dark line is the contrast measured when the prism separation in path II is 0 mm, and the light line is the contrast measured when the prism separation in path I is set to 4 mm. We see that the two curves are the same (within experimental errors) simply shifted relative to each other by 4 mm. This shows that indeed the loss of the contrast can be recovered and is not due to decoherence inside the interferometer.

the wave function of the neutrons as a plane wave and integrating over the vertical momentum distribution. In these simulations we used the vertical momentum distributions shown in Fig. 3(a). Plane wave simulations are a good approximation to the measured contrast behavior. As we mentioned above, any single crystal irregularities are not affecting our measurements of the coherence length. To demonstrate that the observed loss of contrast is not due to decoherence related to the vertical beam displacement we recover the contrast by shifting the path of the neutron beam in path II in the same direction as in path I (Fig. 4). Here we first shift the beam in path I vertically while maintaining the position of the beam in path II. To do that we separate the prisms in path I gradually from 0 mm to 4 mm which shifts the beam up while keeping the prisms in path II together (separation = 0). The dark line and top axis shows the contrast change due to this separation. We see that at a position around -3 mm we completely loose the interferometer contrast. Then we fixed the separation of the prisms in path I and separated the prisms in path II such that the beam in path II is shifted in the same (up) direction. The light curve and bottom axis represent the contrast while separating the prisms in path II. We observe that the light curve follows the dark one within the error-bars. Thus we can refocus the lost contrast and confirm that loss of contrast is due to the separation of the beams.

Conclusion.—We have measured the vertical coherence function of a single crystal neutron interferometer via path separation and for different vertical beam momentum distributions. We extended this measurement to separations up to 1000 Å. In one of the beam configurations (single blade monochromator) we observed a coherence length of 788 Å. Having a single crystal neutron interferometer with a long coherence length provides new opportunities for experiments such as Fourier Spectroscopy. Finally, we show that the loss of coherence due to path displacement is fully recovered by displacing the second path the corresponding distance.

Financial support provided by NIST and the Department of Energy's INIE program is gratefully acknowledged. The authors are grateful for discussions with D. L. Jacobson, C. Ramanathan, B. Levi, D. Hussey, R. Barankov.

*mitja@mit.edu

[1] L. Mandel and E. Wolf, *Optical Coherence and Quantum Optics* (Cambridge University Press, Cambridge, England, 1995).
[2] M. Suda, *Quantum Interferometry in Phase Space: Theory And Applications* (Springer, New York, 2006).
[3] U. Bonse and E. te Kaat, Z. Phys. **243**, 14 (1971).
[4] P. Becker and U. Bonse, J. Appl. Crystallogr. **7**, 593 (1974).
[5] H. Rauch, Physica (Amsterdam) **213–214B**, 830 (1995).
[6] A. J. Leggett, *The Lessons of Quantum Theory*, edited by J. de Boer, E. Dal, and O. Ulfbeck (Elsevier, Amsterdam, 1986).
[7] H. Rauch and S. A. Werner, *Neutron Interferometry* (Oxford University Press, New York, 2000).
[8] H. Rauch, H. Wölwitsch, H. Kaiser, R. Clothier, and S. A. Werner, Phys. Rev. A **53**, 902 (1996).
[9] Chapter 4, *Coherence properties*, in [7].
[10] M. Arif, D. E. Brown, G. L. Greene, R. Clothier, and K. Littrell, Proc. SPIE Int. Soc. Opt. Eng. **2264**, 20 (1994).
[11] K. Schoen, D. L. Jacobson, M. Arif, P. R. Huffman, T. C. Black, W. M. Snow, S. K. Lamoreaux, H. Kaiser, and S. A. Werner, Phys. Rev. C **67**, 044005 (2003).